

# The compression yield behaviour of polymethyl methacrylate over a wide range of temperatures and strain-rates

C. BAUWENS-CROWET

*Institut des Matériaux, Université libre de Bruxelles, Bruxelles, Belgium*

The compression yield behaviour of PMMA has been investigated, here, over a wide range of experimental conditions which cannot be reached in tensile tests owing to the brittle nature of the material. The plot of the ratio of the compression yield stress to absolute temperature, as a function of the logarithm of the strain-rate, gives a set of parallel curves which can be accurately superimposed by shifting along a slanting straight line. A master curve is built from which the yield behaviour may be predicted for any state of stress, or value of temperature and strain-rate in the glassy range, using Bauwens' yield criterion.

The validity of the procedure is checked for compression tests at low temperatures, for tensile tests in the range of experimental conditions where PMMA yields and for torsional tests under hydrostatic pressure (data of Ward *et al*). In every case, the fit is found to be quite accurate.

A region of experimental conditions is determined where the compression yield behaviour may not be described by the Ree-Eyring treatment involving a hyperbolic sine function. In this region, the Bauwens approach, which consists of a modification of the Ree-Eyring theory, taking into account a distribution of relaxation times and linking the yield behaviour with the  $\beta$  mechanical loss peak, is found to give an acceptable fit to the data.

## 1. Introduction

The yield behaviour of polymethyl methacrylate (PMMA) has been investigated in uniaxial compression tests over four decades of strain-rates at temperatures in the range of ( $-20$  to  $100^\circ\text{C}$ ), and also at one strain-rate, from ( $-80$  to  $100^\circ\text{C}$ ).

The plot of  $|\sigma_c|/T$  (ratio of compression yield stress to absolute temperature) as a function of  $\log \dot{\epsilon}$  (ratio of strain-rate at several constant temperatures, gives a family of parallel curves (one curve for each temperature). Careful examination of the graph led us to draw the following conclusions:

(a) the set of curves can be looked upon as being shifted by the shift of one curve along a slanting straight line, locus of the intersections of the asymptotes of each curve;

(b) the shift factor along this straight line

accurately fits the Arrhenius relation. Therefore a master curve can be built.

Starting from these important experimental features, we decided not to describe the compression yield behaviour of PMMA by the modified Robertson model, developed by Ward *et al* [1], because this treatment does not imply such consequences. On the other hand, it must be noted that over a relatively wide region, the master curve exhibits an appreciable curvature. In this region, the data do not accurately fit the Ree-Eyring equation [2] which, at first sight, seemed to agree with the tensile yield stress data of PMMA [3, 4]. On the contrary, the compression data obtained here, are in agreement with a hypothetical mechanism of yielding proposed by Bauwens [5, 6] which is useful to describe the yield behaviour of polyvinylchloride (PVC) and polycarbonate (PC), in compression as well as in

tensile tests. Bauwens' approach is based on the Ree-Eyring theory; furthermore it correlates the yield stress with the mechanical damping peaks observed in glassy polymers, and establishes a yield criterion [7, 8] which is temperature, strain-rate and pressure dependent.

We agree with Ward [9] in that this treatment is not so elaborate as the attractive Robertson theory [10], but it has the merit of accounting for a number of different aspects of yield properties, and the accuracy of the fit to the data is fairly good over a wide range of experimental conditions.

We intend, here, to

1. give a master curve related to the variation of the yield stress of PMMA in uniaxial compression tests, as a function of logarithm of strain-rate;
2. check Bauwens' yield criterion using compression and tensile data as well as values of the torsional yield stress under hydrostatic pressure (measurements of Ward *et al* [11]);
3. correlate the yield behaviour with the  $\beta$  mechanical loss peak observed in damping tests, following a treatment first proposed by Bauwens for PVC and PC [5, 6];
4. show that the interpretation of the tensile yield behaviour of PMMA, given a few years ago, in our laboratory [3] and, independently, by Roetling [4], was partially wrong. An apparently good agreement between the tensile yield stress data and the Ree-Eyring theory was then obtained because of the narrow range of experimental conditions where PMMA yields in tensile tests.

## 2. Experimental

Commercially-available PMMA (Perspex ICI) in the form of sheets 5 mm thick, was used. The equipment used to obtain compression and tensile yield stresses, and the shape and the dimensions of the test pieces, were described previously [12].

Over the whole range investigated, load-extension curves exhibit a well-defined maximum at a few per cent strain. This maximum is taken as the yield point; the corresponding load is denoted by  $F$ . The yield stress was calculated using the following equations, respectively valid in tensile and compression tests:

$$\sigma_t = \frac{F}{S_0} (1 + e) \quad (1)$$

$$|\sigma_c| = \frac{F}{S_0} (1 - e) \quad (2)$$

where  $\sigma$  is the corrected yield stress,  $S_0$  the initial cross-section and  $e$  the measured strain corresponding to  $F$ . This manner of evaluating the yield stresses is implied by Bauwens' treatment, as already discussed in a previous paper [12].

The damping tests were performed using a torsion pendulum placed in an environmental chamber. The loss tangent was measured from ( $-80$  to  $90^\circ\text{C}$ ), on a specimen  $10\text{ cm} \times 1.5\text{ cm} \times 0.2\text{ cm}$ . The pendulum was set, at room temperature, at two different frequencies around 1 cps, namely: 0.46 and 1.82 cps.

## 3. Results

### 3.1. Compression yield stresses

The plot of  $|\sigma_c|/T$  versus  $\log \dot{\epsilon}$  (where  $\dot{\epsilon}$  is the strain-rate) is shown in Fig. 1.

The graph shows the set of parallel curves which agrees with the data and satisfies the following conditions:

1. the set of curves must be generated by the shift of any curve along a slanting straight line (called  $d_c$ );
2. the shift factor along  $d_c$  must fit an Arrhenius equation. From this graph we have built a master curve, reduced to  $100^\circ\text{C}$ , which is shown in Fig. 2 (full curve).

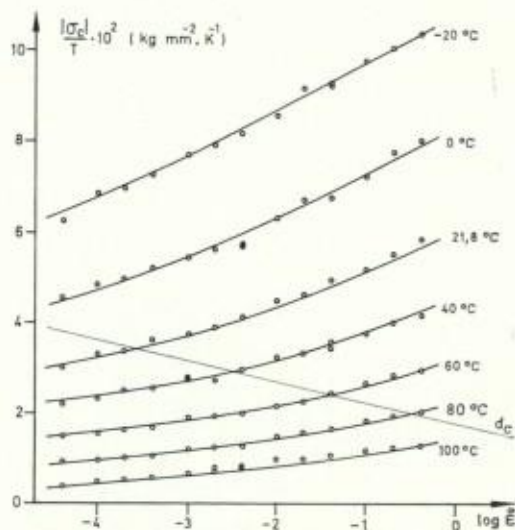


Figure 1 Ratio of compression yield stress to temperature as a function of logarithm of strain-rate. The set of curves is generated by the shift of one curve along  $d_c$ , according to Equation 7. ( $\dot{\epsilon}$  in  $\text{sec}^{-1}$ .)

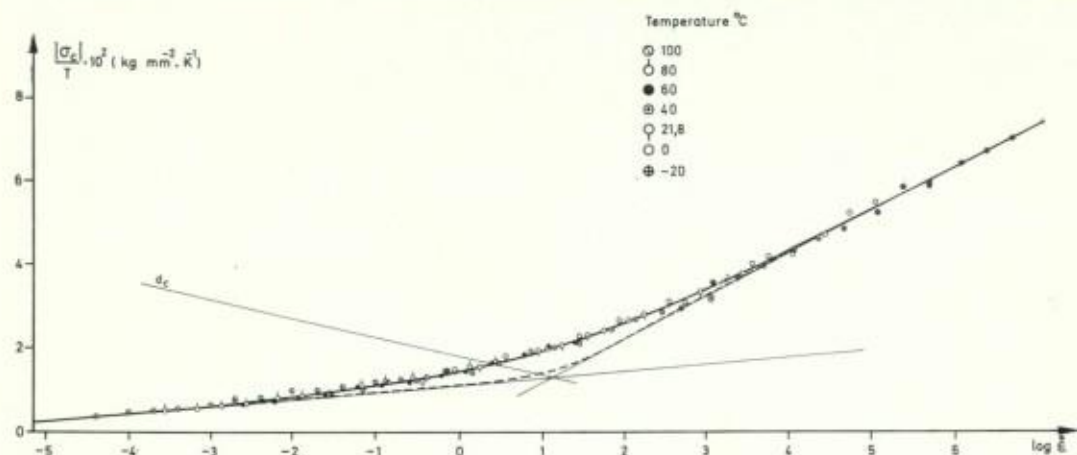


Figure 2 Master compression yield stress curve reduced to 100°C (full curve). The asymptotes are expressed by Equations 3 and 4. The dashed curve is calculated from the Ree-Eyring equation (8).

If one assumes that two rate processes,  $\alpha$  and  $\beta$ , are involved in the deformation at yield, the Ree-Eyring theory as well as Bauwens' treatment predict that the asymptotes of a given curve are expressed by

$$\left\{ \frac{|\sigma_c|}{T} = A_{c\alpha} \left( \ln 2 C_\alpha \dot{\epsilon} + \frac{Q_\alpha}{RT} \right) \right\} \dot{\epsilon}_x \leq \dot{\epsilon} \leq \dot{\epsilon}_\beta \quad (3)$$

and

$$\left\{ \frac{|\sigma_c|}{T} = A_{c\alpha} \left( \ln 2 C_\alpha \dot{\epsilon} + \frac{Q_\alpha}{RT} \right) + A_{c\beta} \left( \ln 2 C_\beta \dot{\epsilon} + \frac{Q_\beta}{RT} \right) \right\} \dot{\epsilon} > \dot{\epsilon}_\beta \quad (4)$$

where  $A_{c\alpha}$ ,  $A_{c\beta}$  are constants;  $C_\alpha$  and  $C_\beta$  are constants containing a frequency factor;  $Q_\alpha$  and  $Q_\beta$  are the activation energies related to the  $\alpha$  and  $\beta$  processes respectively, and  $R$  denotes the universal gas constant.  $\dot{\epsilon}_\beta$  is the value of the strain-rate corresponding to the intersection of the two asymptotes and  $\dot{\epsilon}_x$  the value of the strain-rate obtained by extrapolating the curve to zero stress. It follows that

$$\dot{\epsilon}_\beta = \frac{1}{2 C_\beta} \exp \left( - \frac{Q_\beta}{RT} \right) \quad (5)$$

and

$$\dot{\epsilon}_x = \frac{1}{2 C_\alpha} \exp \left( - \frac{Q_\alpha}{RT} \right). \quad (6)$$

Let us consider two curves belonging to the family shown in Fig. 1 and related to temperature  $T_1$  and  $T_2$ , respectively, and let  $s_x(T_1, T_2)$  denote the horizontal component of the shift factor

between these two curves; it therefore follows from both treatments that

$$s_x(T_1, T_2) = \frac{Q_\beta}{2.303 R} \left( \frac{1}{T_1} - \frac{1}{T_2} \right). \quad (7)$$

The values of the parameters were estimated from Fig. 1 and from the best fit of Equations 3, 4 and 7 to the data of Figs. 1 and 2; they are given in Table I. The procedure followed is described in the Appendix.

TABLE I Parameters calculated from the fit of Equations 3, 4, 7 and 9 to the data.

$\alpha$ process	$\beta$ process
$Q_\alpha = 98.5 \text{ kcal mol}^{-1}$	$Q_\beta = 25.6 \text{ kcal mol}^{-1}$
$C_\alpha = 5 \times 10^{-32} \text{ sec}$	$C_\beta = 4.67 \times 10^{-17} \text{ sec}$
$A_{c\alpha} = 7.1 \times 10^{-4} \text{ kg mm}^{-2} \text{ K}^{-1}$	$A_{c\beta} = 3.74 \times 10^{-3} \text{ kg mm}^{-2} \text{ K}^{-1}$
$A_{t\alpha} = 5.5 \times 10^{-4} \text{ kg mm}^{-2} \text{ K}^{-1}$	

The Ree-Eyring equation may be written as follows:

$$\frac{|\sigma_c|}{T} = A_{c\alpha} \left( \ln 2 C_\alpha \dot{\epsilon} + \frac{Q_\alpha}{RT} \right) + A_{c\beta} \sinh^{-1} \left( C_\beta \dot{\epsilon} \exp \frac{Q_\beta}{RT} \right). \quad (8)$$

Using the values given in Table I, the dashed curve in Fig. 2 was calculated from Equation 8. It can easily be seen from the graph that this curve does not give an acceptable fit to the data when ( $1 \leq \log \dot{\epsilon} \leq 3$ ).

The theoretical expression of the full curve in

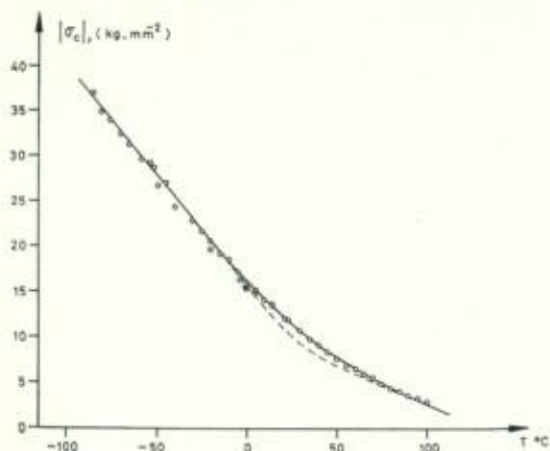


Figure 3 Plot of the compression yield stress versus temperature at a constant strain-rate,  $\dot{\epsilon} = 4.16 \times 10^{-3} \text{ sec}^{-1}$ . The full curve is deduced from the master curve of Fig. 2; the dashed curve is calculated from Equation 8; both curves have the same asymptotic limits.

Fig. 2, as a function of the  $\beta$  mechanical loss peak, may be obtained by using a procedure similar to that given in ref. [6], but initially, we have considered this curve as a semi-empirical one, from which, using Bauwens' criterion, we intend to predict the yield behaviour of PMMA in the glassy range, for an arbitrary state of stress, or value of strain-rate or temperature. For example, in order to check the value of the compression yield stress at low temperatures implied by this master curve, we have deduced from it another curve representing  $|\sigma_c|$  as a

function of temperature at a constant strain-rate:  $\dot{\epsilon} = 4.16 \times 10^{-3} \text{ sec}^{-1}$ . This latter curve is given in Fig. 3, where it is seen that there is a fairly good fit to the data.

### 3.2. Tensile yield stresses

The plot of  $\sigma_t/T$  (ratio of tensile yield stress to absolute temperature) versus  $\log \dot{\epsilon}$  is shown in Fig. 4. Since PMMA usually fractures before yielding, when tested at moderate-to-high strain-rates below 50°C, the obtained data do not cover a wide range of experimental conditions. A set of parallel curves is drawn through the points in such a way that:

1. the extrapolation for small stresses of the curve related to  $T = 100^\circ\text{C}$  meets the horizontal axis at a point having an abscissa equal to  $\log \dot{\epsilon}_x$  (same value as in Fig. 2);
2. the family of curves is generated by the shift of any curve along a slanting line (called  $d_t$ ); and
3. Equation 7 is satisfied although the shift is carried out along  $d_t$  instead of  $d_c$ .

A master curve, reduced to  $100^\circ\text{C}$ , is built from Fig. 4 and is given in Fig. 5. The procedure followed implies that  $\dot{\epsilon}_\beta$  has the same value in Fig. 2 as in Fig. 5, but in the latter case, it is seen that only one asymptote (related to the small stresses) can be drawn through the points. This asymptote is expressed by:

$$\left\{ \frac{\sigma_t}{T} = A_{tx} \left( \ln 2 C_x \dot{\epsilon} + \frac{Q_x}{RT} \right) \right\}_{\dot{\epsilon}_x \leq \dot{\epsilon} \leq \dot{\epsilon}_\beta} \quad (9)$$

where  $A_{tx}$  is a constant. Its value, estimated from

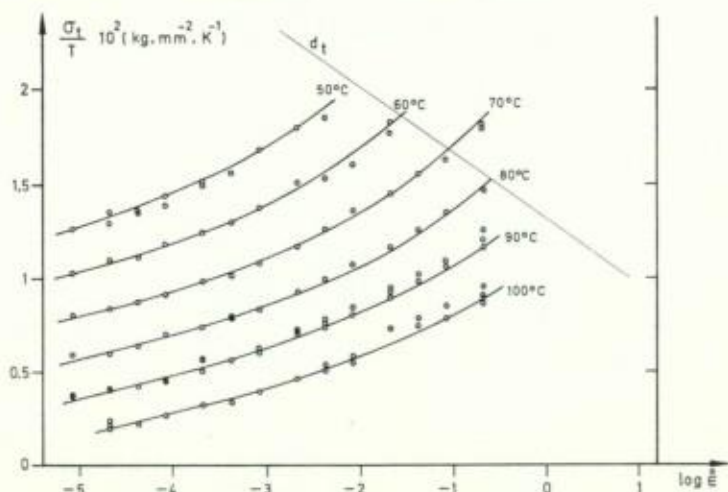


Figure 4 Ratio of tensile yield stress to temperature as a function of logarithm of strain-rate. The set of curves is generated by the shift of one curve along  $d_t$  according to Equation 7. ( $\dot{\epsilon}$  in  $\text{sec}^{-1}$ .)

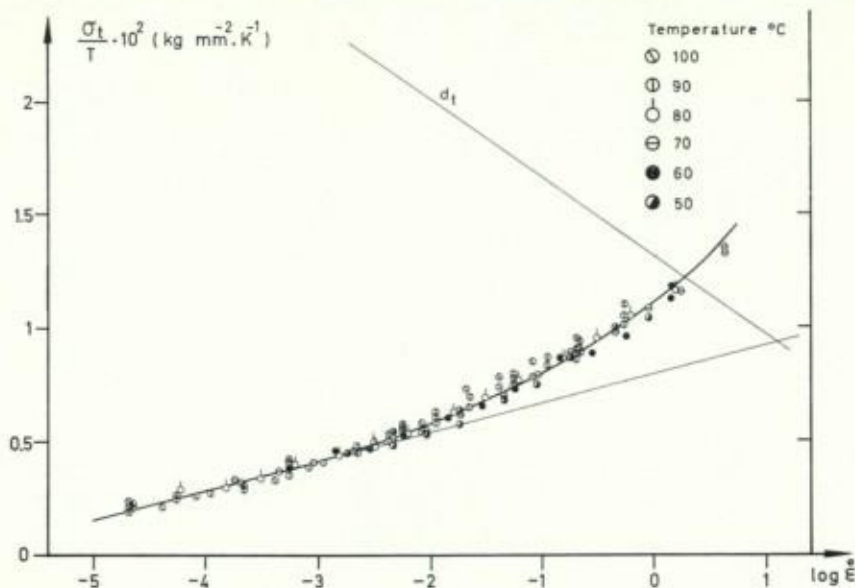


Figure 5 Master tensile yield stress curve reduced to 100°C. The asymptote of the curve is expressed by Equation 9 where  $\dot{\epsilon}_\alpha$  and  $\dot{\epsilon}_\beta$  have the same value as in Equations 3 and 4.

the best fit of Equation 9 to the data, is given in Table I.

### 3.3. Mechanical damping tests

The results of the damping tests are shown in Fig. 6, where the loss tangent ( $\tan \delta$ ), is plotted versus temperature. A broad asymmetric peak is found.

It must be noted that the maximum value of  $\tan \delta$  rises slightly with increasing frequency, indicating that the observed peak is the combination of two or more component peaks [13]. Owing to this fact, the case of PMMA is more complicated than those of PVC [5] and PC [6], where a single peak, having the same activation energy as that of the  $\beta$  process, was found at low temperatures. It was, therefore, necessary to split the measured peak, in order to isolate the component which we intend to relate to the compression yield stress curves of Figs. 2 and 3.

A hypothetical split is given in Fig. 7, where the components have the following characteristics:

1. the shift of the maximum of the  $p_1$  component, from  $p_{1a}$  to  $p_{1b}$ , corresponds to an activation energy equal to that of the  $\beta$  process, i.e. 25.6 kcal mol<sup>-1</sup> (see Table I);
2. the existence of a symmetric peak,  $p_2$ , is assumed, whose maximum is located at 65°C and whose shift is negligibly small for the

variation of frequency considered here. This peak may perhaps be associated with the  $\alpha'$  transition revealed by Thompson [14]; and  
3. the peak related to the main transition of PMMA is also supposed to interfere by means of its low temperatures wing:  $p_3$ .

The addition of peaks  $p_{1a}$ ,  $p_2$ ,  $p_3$  and  $p_{1b}$ ,  $p_2$ ,  $p_3$

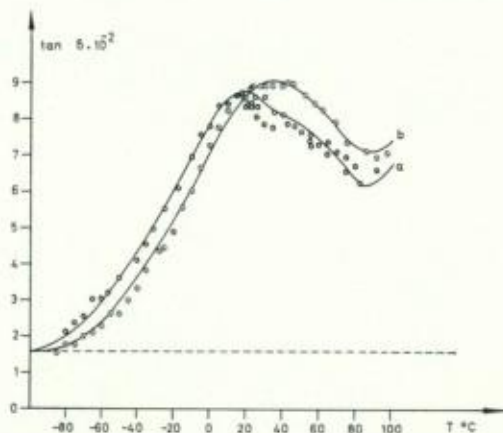


Figure 6 Loss tangent of PMMA as a function of temperature in the  $\beta$  transition range. Curves a and b are the combination of the hypothetical peaks  $p_{1a}$ ,  $p_2$ ,  $p_3$  and  $p_{1b}$ ,  $p_2$ ,  $p_3$  of Fig. 7. The frequency varied from 0.62 to 0.36 cps (data related to curve a) and from 2.4 to 1.5 cps (data related to curve b).

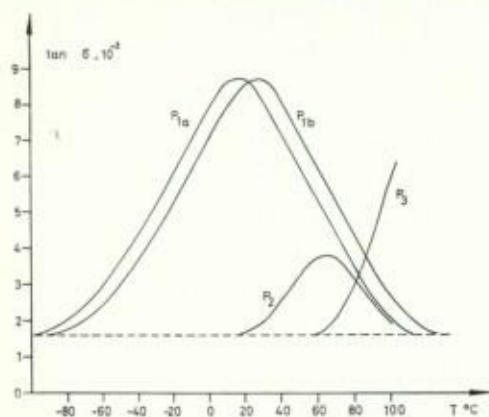


Figure 7 Hypothetical components of the curves a and b given in Fig. 6. The shift of the maximum of peak  $p_1$  from  $p_{1a}$  to  $p_{1b}$  is related to an activation energy equal to  $Q_\beta$ . Peaks  $p_2$  and  $p_3$  are supposed to be fixed.

gives rise to the curves a and b, respectively (Fig. 6), which are in agreement with the data.

#### 4. Interpretation

##### 4.1. Relation between the compression, tensile and torsional yield stresses

It has been shown previously [12], that Bauwens' criterion must be applied separately to the  $\alpha$  and the  $\beta$  processes. Let  $|\sigma_{c\alpha}|$ ,  $|\sigma_{c\beta}|$  and  $\sigma_{t\alpha}$ ,  $\sigma_{t\beta}$  be the  $\alpha$  and  $\beta$  contributions to the compression and tensile yield stresses, respectively. The expression of  $|\sigma_{c\alpha}|$  and  $\sigma_{t\alpha}$  is supposed to be

$$|\sigma_{c\alpha}| = A_{c\alpha} T \left( \ln 2 C_\alpha \dot{\epsilon} + \frac{Q_\alpha}{RT} \right) \quad (10)$$

and

$$\sigma_{t\alpha} = A_{t\alpha} T \left( \ln 2 C_\alpha \dot{\epsilon} + \frac{Q_\alpha}{RT} \right). \quad (11)$$

Values of  $|\sigma_{c\beta}|$  and  $\sigma_{t\beta}$  are obtained by subtracting  $|\sigma_{c\alpha}|$  or  $\sigma_{t\alpha}$  (as expressed by Equations 10 or 11) from the  $|\sigma_c|$  and  $\sigma_t$  (as measured or extrapolated from the master curves).

Although Bauwens' yield criterion is temperature and strain-rate dependent, it leads to the following equations:

$$\frac{|\sigma_{c\alpha}|}{\sigma_{t\alpha}} = \frac{\sqrt{2 + \mu}}{\sqrt{2 - \mu}} = \frac{A_{c\alpha}}{A_{t\alpha}} \quad (12)$$

and

$$\frac{|\sigma_{c\beta}|}{\sigma_{t\beta}} = \frac{\sqrt{2 + \mu'}}{\sqrt{2 - \mu'}} = \frac{A_{c\beta}}{A_{t\beta}} \quad (13)$$

where  $\mu$  and  $\mu'$  are constants. Plots of  $|\sigma_{c\alpha}|$

TABLE II Parameters determined by fitting the yield criterion to compression and tensile data

$\alpha$ process	$\beta$ process
$\mu = 0.178$	$\mu' = 0$
$A_\alpha = 3.58 \times 10^{-4} \text{ kg mm}^{-2} \text{ K}^{-1}$	$A_\beta = 2.16 \times 10^{-3} \text{ kg mm}^{-2} \text{ K}^{-1}$
Comparison between theoretical and measured values of $\tau$ (same experimental conditions: atmospheric pressure, $\dot{\gamma} = 4 \times 10^{-4} \text{ sec}^{-1}$ , $T = 25^\circ \text{C}$ ).	
Calculated from Equations 15 and 16	Data of Ward <i>et al</i> [11] $\tau = 5.12 \text{ kg mm}^{-2}$
$\tau = \tau_\alpha + \tau_\beta = 4.94 \text{ kg mm}^{-2}$	

versus  $\sigma_{t\alpha}$  and  $|\sigma_{c\beta}|$  versus  $\sigma_{t\beta}$  are given in Fig. 8a and b, respectively; values of  $\mu$  and  $\mu'$ , calculated from the fit of relations 12 and 13 to the data, are presented in Table II.

As  $\mu'$  was found equal to zero for PMMA, it follows from Equation 13 that

$$A_{c\beta} = A_{t\beta}. \quad (14)$$

Now, let  $\tau$  and  $\dot{\gamma}$  denote the yield stress and the shear-rate related to torsional stress-strain tests, respectively. If the torsional tests are performed at atmospheric pressure at a shear-rate equivalent to  $\dot{\epsilon}$ , the  $\alpha$  and  $\beta$  components of  $\tau$  may be expressed as a function of  $|\sigma_{c\alpha}|$  and  $|\sigma_{c\beta}|$ , respectively, using Bauwens' criterion. This author considers that strain-rates are equivalent if they produce, during the same time, plastic strains corresponding to the same value of the first strain invariant [7, 8]. Therefore, torsional and compression yield stresses are related to equivalent strain-rates when  $\dot{\gamma} = \sqrt{3} \dot{\epsilon}$ , and it follows that

$$\tau_\alpha = A_\alpha T \left( \ln \frac{2 C_\alpha \dot{\gamma}}{\sqrt{3}} + \frac{Q_\alpha}{RT} \right) = \frac{A_\alpha}{A_{c\alpha}} |\sigma_{c\alpha}| \quad (15)$$

and

$$\tau_\beta = \frac{A_\beta}{A_{c\beta}} |\sigma_{c\beta}| \quad (16)$$

where  $A_\alpha$  and  $A_\beta$  are constants such that

$$A_\alpha = \frac{2A_{c\alpha}}{\sqrt{3} \left( 1 + \frac{A_{c\alpha}}{A_{t\alpha}} \right)} \quad (17)$$

and

$$A_\beta = \frac{2A_{c\beta}}{\sqrt{3} \left( 1 + \frac{A_{c\beta}}{A_{t\beta}} \right)}. \quad (18)$$

From these equations, a value of  $\tau = \tau_\alpha + \tau_\beta$  under atmospheric pressure, is calculated for  $T = 25^\circ\text{C}$  and  $\dot{\gamma} = 4 \times 10^{-4} \text{ sec}^{-1}$ , the result is given in Table II, where it is compared with the data of Ward *et al* [11] obtained under the same conditions.

Bauwens' criterion predicts that the dependence of  $\tau_\alpha$  and  $\tau_\beta$  on hydrostatic pressure ( $-p$ ), for tests performed at constant strain-rate and temperature is given by

$$\tau_\alpha + \frac{3}{\sqrt{6}} \mu(-p) = \text{constant} \quad (19)$$

and

$$\tau_\beta + \frac{3}{\sqrt{6}} \mu'(-p) = \text{constant}. \quad (20)$$

The variation of  $\tau$  with ( $-p$ ) was calculated from Equations 19 and 20 and plotted in Fig. 8c, where it is compared with the data of Ward *et al* [11]. The accuracy of the fit is satisfactory.

#### 4.2. Correlation between compression yield behaviour and the $\beta$ loss peak

Bauwens' treatment states that the molecular movement related to the  $\beta$  process considered in the Ree-Eyring theory is that which is associated with the  $\beta$  mechanical loss peak. For an initial approach, let us assume that the  $\beta$  mechanical

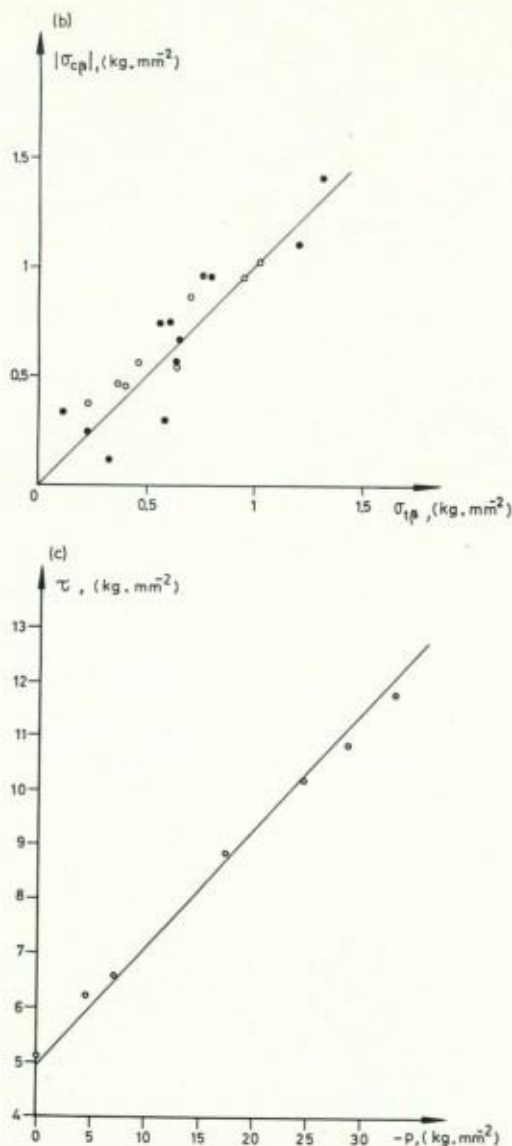


Figure 8 (a) Plot of the compression yield stress versus tensile yield stress, in the range of experimental conditions where only the  $\alpha$  process is involved in the deformation. The straight line drawn on the graph is calculated from Equation 12 using Table I. (b) Plot of the  $\beta$  contribution to the yield stress in compression versus the  $\beta$  contribution in tension (full circles: both quantities are measured; open circles: one quantity is measured while the other is extrapolated from the master curve). (c) Torsional yield stress as a function of pressure ( $T = 25^\circ\text{C}$ ,  $\dot{\gamma} = 4 \times 10^{-4} \text{ sec}^{-1}$ ). (Data of Ward *et al* [11]). The straight line drawn on the graph is calculated from Equations 19 and 20 using Table II.

loss peak of PMMA is  $p_1$  (Fig. 7). Bauwens correlates this peak to the relaxation spectrum,  $H(-\ln \omega_\beta)$  corresponding to the  $\beta$  transition range. Let  $\Delta \ln \omega_\beta$  denote the half-width value of the spectrum;  $\omega_\beta$  is the characteristic radian frequency of a given element whose response to free oscillation tests may be calculated using the three element model of Fig. 9.

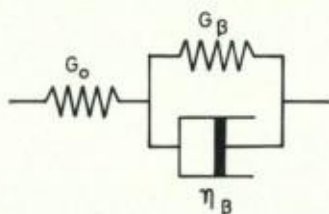


Figure 9 Simple three-element model used in Bauwens' treatment.

Taking the following expression for  $\omega_\beta$  [6]:

$$\omega_\beta = \frac{G_\beta}{\eta_\beta} = \frac{\sqrt{3} G_\beta}{A_\beta C_\beta T} \exp\left(-\frac{Q_\beta}{RT}\right) \quad (21)$$

where  $\eta_\beta$  is the Newtonian viscosity of the viscous element and  $G_\beta$  is a constant, it is seen that a distribution of  $\ln \omega_\beta$  can arise from a distribution in the value of either  $C_\beta$  or  $Q_\beta$ . The latter case was found to give a good basis for describing the yield behaviour of PVC and PC [5, 6]. Data obtained on PMMA allow one to check, over a wide range of experimental conditions, that the curves of Figs. 1 or 4 can accurately be superimposed even in the region where they exhibit a definite curvature. The superimposability of the data in such regions

implies that the dependence of the yield behaviour on an activation energy spectrum may be neglected initially. Therefore, we will consider here that  $H(-\ln \omega_\beta)$  arises from a distribution in the values of  $C_\beta$ . Let this distribution function be expressed by

$$\int_0^\infty P(\ln C_\beta) d \ln C_\beta = 1. \quad (22)$$

It can be derived from Equation 21 that

$$d \ln \omega_\beta = -d \ln C_\beta. \quad (23)$$

a relation which allows the half width value of  $P(\ln C_\beta)$  to be taken as equal to  $\Delta(\ln \omega_\beta)$ .

The expression of  $\tan \delta$  (approximation of first order) given in Bauwens' treatment, may be rewritten in terms of a distribution in the values of  $C_\beta$

$$\tan \delta = \frac{\pi G_0 P(\ln C)_\beta}{2G_\beta} \quad (24)$$

where  $G_0$  is the shear modulus when both  $\alpha$  and  $\beta$  processes are frozen in. Therefore, from Equations 5, 21 and 24, an equation may be established between, on the one hand, the value of  $\nu_{\max}$  (i.e. the frequency corresponding to the maximum value of the loss tangent, for tests performed at various frequencies at a given temperature), and, on the other hand, the value of  $\dot{\epsilon}_\beta$  related to the same temperature.

$$\nu_{\max} T = \frac{\sqrt{3} G_0}{2A_\beta (\tan \delta)_{\max} \Delta(\ln \omega_\beta)} \dot{\epsilon}_\beta \quad (25)$$

where  $1/[\Delta(\ln \omega_\beta)]$  is approximately the maximum value of  $P(\ln C_\beta)$ . Unfortunately, we are not able to measure  $\tan \delta$  as a function of frequency at constant temperature, a measure-

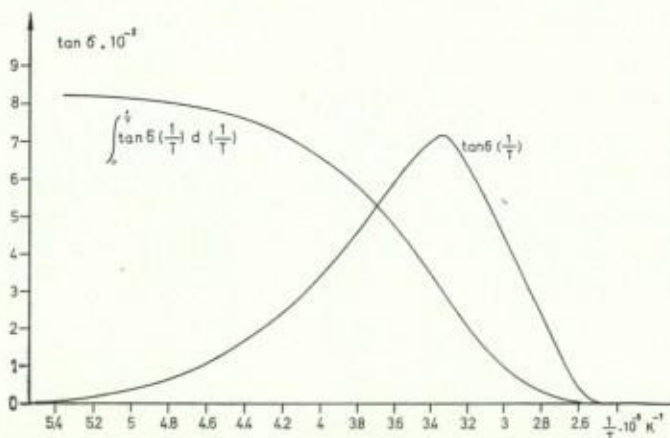


Figure 10 Contribution of peak  $p_{10}$  to the  $\tan \delta (1/T)$  curve and integral of this contribution from 0 to  $1/T$ .



ment which allows the direct evaluation of  $\Delta(\ln \omega_\beta)$ ; but using peak  $p_{1b}$ , for example, we can obtain a plot of  $\tan \delta$  versus  $1/T$  (see Fig. 10.)

Provided that the condition

$$\nu T = \text{constant} \quad (26)$$

is satisfied for every point of the curve (which is approximately true for this peak), it may be derived from Equation 21 that

$$d \ln C_\beta = -\frac{Q_\beta}{R} d(1/T) \quad (27)$$

and, therefore, the half-width value of  $P(\ln C_\beta)$  may be obtained from the half-width value  $\Delta(1/T)$  of the peak given in Fig. 10.

Equation 25 may be rewritten

$$\nu_{\max} T_{\max} = \frac{\sqrt{3} G_0 R}{2A_\beta (\tan \delta)_{\max} Q_\beta \Delta(1/T)} \dot{\epsilon}_\beta \quad (28)$$

In this last equation,  $T_{\max}$  denotes the temperature at which the loss tangent reaches its maximum value, for tests performed at a frequency equal to  $\nu_{\max}$ , as well as the temperature at which the imposed strain-rate, in a tensile or compression test, equals  $\dot{\epsilon}_\beta$ . For example, in the case of uniaxial compression tests performed over a wide range of temperatures and at constant strain-rate  $\dot{\epsilon} = 4.16 \times 10^{-3} \text{ sec}^{-1}$ , the value of  $T$  which satisfies Equation 5 for  $\dot{\epsilon} = \dot{\epsilon}_\beta$  is  $T_{\max} = 29^\circ 3 = 302 \text{ K}$ . The corresponding value of  $\nu_{\max}$  may be calculated from Equation 28 using Table III, if one assumes that  $(\tan \delta)_{\max}$  and  $\Delta(1/T)$  do not depend on the location of the peak, and, therefore, can be evaluated from Fig. 10.

TABLE III Constants of Equation 28

Constants	Determination	Value
$(\tan \delta)_{\max}$	From peak $p_1$ (the value of the background has been subtracted)	$7.15 \times 10^{-2}$
$\Delta(1/T)$	From Fig. 10.	$1.06 \times 10^{-3} \text{ K}^{-1}$
$G_0$	From data of Heijboer [17]	$260 \text{ kg mm}^{-2}$
$Q_\beta$ and $A_\beta$	Are given in Tables I and II, respectively	

The obtained value,  $\nu_{\max} = 1.57 \text{ cps}$ , is close to the measured value,  $\nu_{\max} = 1.79 \text{ cps}$ , related to peak  $p_{1b}$  whose maximum is precisely located at  $T_{\max} = 302 \text{ K}$ . The last two values of frequency and temperature satisfy Equation 28. Although much rough approximation has been

made, we may then conclude that Bauwens' treatment may be applied to correlate the yield stress curve of Fig. 3 to the peak  $p_{1b}$ . In order accurately to check this treatment, we have plotted, in Fig. 11, the  $\beta$  contribution to the compression yield stress versus temperature; the data, as well as the full curve which is, therefore, deduced from the compression master curve, are obtained from Fig. 3.

Following a derivation similar to that of Bauwens,  $|\sigma_{c\beta}|/T$  may be expressed as a function of  $P(\ln C_\beta)$  by

$$\frac{\partial |\sigma_{c\beta}|}{\partial T} = K \int_{\ln C_{\beta T}}^{\infty} P(\ln C_\beta) d \ln C_\beta \quad (29)$$

where  $K$  is a constant and  $C_{\beta T}$  is related to the frequency factor of an element whose  $\beta$  transition occurs at temperature  $T$ . Taking into account Equation 27, Equation 29 may be rewritten

$$\frac{\partial |\sigma_{c\beta}|}{\partial T} = K \frac{\int_0^{1/T} P(1/T) d 1/T}{\int_0^{\infty} P(1/T) d 1/T} \quad (30)$$

which leads to the following expression:

$$|\sigma_{c\beta}| = B_c \int_T^{\infty} dT \int_0^{1/T} P(1/T) d 1/T \quad (31)$$

where  $B_c$  is a constant.

In order to check Equation 31, we have integrated, from 0 to  $1/T$ , the curve of Fig. 10 giving  $\tan \delta$  as a function of  $1/T$  (after subtraction of the background estimated on Fig. 6); the results is also given in Fig. 10. The integral has then been plotted as a function of  $T$  and integrated once again from  $T$  to  $\infty$ . The dashed curve of Fig. 11 is proportional to this double integral and therefore represents Equation 31; the constant was chosen to obtain a coincidence at  $T = -80^\circ \text{C}$  for both curves on the graph.

Although the fit of the dashed curve is not perfect, we think it is sufficient, according to the crude approximations made, to conclude that Bauwens' treatment enables one to describe the yield behaviour of PMMA. Obviously, the same treatment may be applied to generate the curve giving the tensile yield stress as a function of temperature, at constant strain-rate. It leads to the following expression:

$$\sigma_{t\beta} = B_t \int_T^{\infty} dt \int_0^{1/T} P(1/T) d 1/T. \quad (32)$$

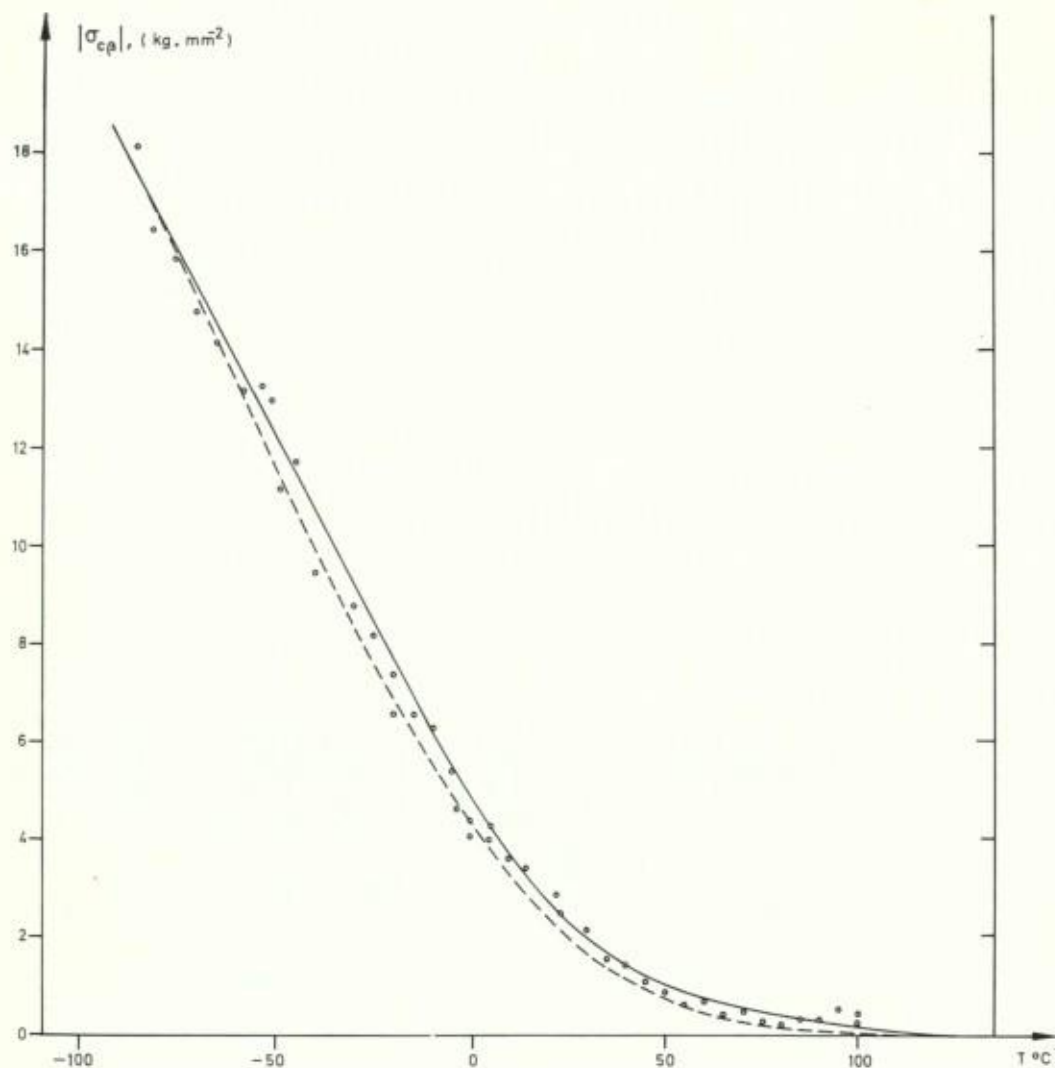


Figure 11  $\beta$  component of the compression yield stress as a function of temperature at constant strain-rate. The data and the full curve are deduced from Fig. 3; the dashed curve is calculated from Equation 31.

## 5. Discussion

It has been pointed out previously [5, 6] that for tensile yield data on PVC and PC, theoretical yield stress curves (i.e.  $\sigma_t = f(T)$ , at constant strain-rate) calculated from the Ree-Eyring equation and from Equation 32, are very close together. Even in the case of compression tests on PC, where Bauwens' treatment gave a quite accurate fit to the data [6], the fit of the Ree-Eyring theory was still acceptable [12].

The present paper shows that for PMMA both treatments differ greatly in the  $\beta$  transition region and that only Bauwens' approach is applicable.

However, an apparent agreement between tensile data and the Ree-Eyring theory was found previously [3, 4]. Comparing Figs. 2 and 5, we understand how important it is that a wide range of strain-rates and temperatures be explored or it may not be possible to determine, with accuracy, the position of the asymptotes of the curves. A wrong position was assigned, previously, which led to values of the constants differing from those presented in Table I. The agreement between the theory and the tensile data merely seemed to be good because of the narrow range of experimental conditions investigated, but

using the parameters thus determined, it is not possible to fit the compression or torsional data presented or recalled here. The derivation followed, links together, quite accurately, the compression, tensile and torsional yield behaviour of PMMA; it is obvious that such a good agreement was obtained by iteration, a procedure which is sometimes long and inconvenient.

The split of the loss tangent peak in order to isolate the  $\beta$  contribution, is certainly highly schematic but relies on the following experimental features:

1. the value of the activation energy  $Q_\beta$  determined from the compression yield data (Table I) and assigned to govern the shift of the maximum of the  $\beta$  peak, is in agreement with results obtained by several authors, among others, Iwayanagi and Hideshima [15], and Thompson [14] (when this last author does not normalize his creep curves by the McCrum and Morris method [16]);

2. the hypothetical existence of the  $p_2$  peak may be supported by the fact that Thompson found a peak (called  $\alpha'$ ) in the same region, but also, that the  $\alpha$  maximum for the isotactic polymer is located at 65°C at 1 cps [17]. As the conventional polymer is about 15% isotactic, peak  $p_2$  may perhaps arise from the presence of the isotactic fraction (with an intensity depending on this fraction). In this case, it is allowable to assume that the shift of  $p_2$  with increasing frequency is negligible compared to that of the  $\beta$  peak.

## 6. Conclusions

In conclusion, it appears that compression and tensile data on PMMA, giving the variation of  $|\sigma_c|/T$  or  $\sigma_t/T$  as a function of the logarithm of strain-rate, can accurately be time-temperature shifted along a slanting straight line. The comparison made between compression, tensile and torsional yield measurements shows that the yield criterion established by Bauwens fits the data fairly well, provided it is applied separately to each of the two kinds of activated rate processes ( $\alpha$  and  $\beta$ ) which are supposed to be involved in the deformation at yield.

Compression data, which cover a wide range of experimental conditions, only fit the Ree-Eyring equation in the case where the approximation that  $\sinh x \approx 1/2 \exp x$ , is valid, and, therefore, indicate that the hyperbolic sine function fails to describe the yield behaviour of PMMA. Bauwens' approach, which may be considered as

a modification of the Ree-Eyring theory providing for a distribution of relaxation times, is found to give an acceptable fit to the yield stress data.

The time-temperature superimposability of the data, in the region where the yield stress curves,  $[|\sigma_c|/T = f(\log \dot{\epsilon})]_{T = \text{const}}$ , exhibit a definite curvature, allows one to neglect the influence of an activation energy spectrum on the yield behaviour and, therefore, to assume that the distribution of relaxation times arises from a distribution in the values of the frequency factors of the  $\beta$  elements.

## Acknowledgements

Grateful acknowledgement is given to Professor G. Homès, Directeur de l'Institut des Matériaux de l'Université libre de Bruxelles, for his interest during the course of this work, and to J. C. Bauwens, Professeur Associé à l'Université libre de Bruxelles, for many helpful comments, discussions and suggestions.

## Appendix

Evaluation of the constants:  $A_{c\alpha}$ ,  $C_\alpha$ ,  $Q_\alpha$  and  $A_{c\beta}$ ,  $C_\beta$ ,  $Q_\beta$

The values of the parameters, reported in Table I, were estimated, as follows, from the data of Fig. 1.

It is first assumed that the curves related to the highest and the lowest temperature regions, reach the asymptote expressed by Equations 3 or 4 respectively, within the explored range of experimental conditions. A set of straight lines is then drawn on a transparency throughout the data related to the highest temperatures and the lowest strain-rates. The mean slope is taken as  $A_{c\alpha}$ .

A set of parallel straight lines having a slope equal to  $A_{c\alpha}$  is tried; from the horizontal shift of these lines and from the extrapolated value of the abscissas for  $|\sigma_c|/T = 0$ , mean values of  $Q_\alpha$  and  $C_\alpha$  are calculated respectively. Then, a set of parallel straight lines (called set  $\alpha$ ) is recalculated from Equation 3 using the mean value of  $Q_\alpha$ ,  $C_\alpha$ ,  $A_{c\alpha}$ , for each temperature from -20 to 100°C, at which the tests have been performed (see Fig. 12).

Another set of straight lines is then tried throughout the data, in the region of Fig. 1, related to the highest strain-rates and the lowest temperatures. From the mean slope,  $A_{c\beta}$  is evaluated. A set of parallel straight lines (called set  $\beta$ ) is drawn which meets set  $\alpha$  in such a way

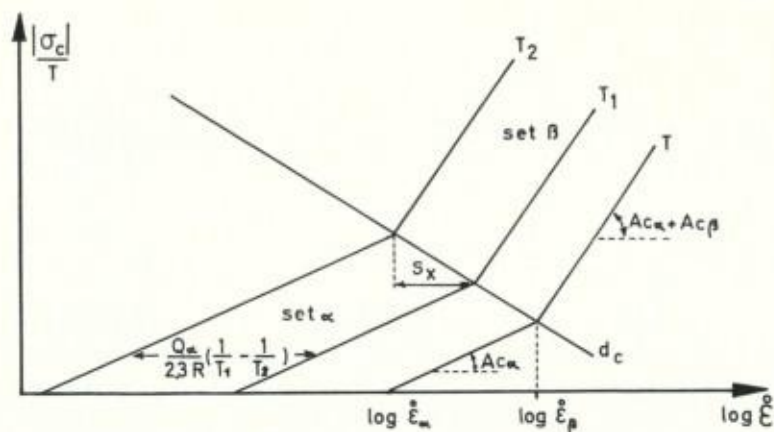


Figure 12 Graphical method of evaluating the constants of Equations 3 and 4 (schematic).

that the locus of the intersections of straight lines, related, in both sets, to the same temperature, is a straight line called  $d_c$  (see Fig. 12). This procedure allows one to consider that the asymptotes, so obtained at each temperature, can be superimposed by a slanting translation along  $d_c$ . From measurements of  $s_x$  (expressed by Equation 7), the horizontal component of the shift factor,  $Q_\beta$  has been evaluated; and from the abscissa of the intersection of two asymptotes at a given temperature,  $C_\beta$  has been calculated using Equation 5.

## References

1. R. A. DUCKETT, S. RABINOWITZ, and I. M. WARD, *J. Mater. Sci.* **5** (1970) 909.
2. T. REE and H. EYRING, in "Rheology", Vol. II, F. R. Eirich, Ed. (Academic Press, New York, 1958), Chapter III.
3. C. BAUWENS-CROWET and G. HOMÈS, *C.R. Acad. Sci. (Paris)* **259** (1964) 3434.
4. J. A. ROETLING, *Polymer* **6** (1965) 311.
5. J. C. BAUWENS, *J. Polymer Sci.* **C33** (1971) 123.
6. *Idem*, *J. Mater. Sci.* **7** (1972) 577.
7. *Idem*, *J. Polymer Sci. A-2*, **5** (1967) 1145.
8. *Idem*, *ibid A-2*, **8** (1970) 893.
9. I. M. WARD, *J. Mater. Sci.* **6** (1971) 1397.
10. R. E. ROBERTSON, *J. Chem. Phys.* **44** (1966) 3950.
11. S. RABINOWITZ, I. M. WARD, and J. S. C. PARRY, *J. Mater. Sci.* **5** (1970) 29.
12. C. BAUWENS-CROWET, J. C. BAUWENS, and G. HOMÈS, *ibid* **7** (1972) 176.
13. G. LOCATI and A. V. TOBOLSKY, *Adv. Mol. Relaxation Processes* **1** (1970) 375.
14. E. V. THOMPSON, *J. Polymer Sci. A-2*, **6** (1968) 433.
15. S. IWAYANAGY and T. HIDESHIMA, *J. Phys. Soc. Japan* **8** (1953) 368.
16. N. G. MCCRUM and E. L. MORRIS, *Proc. Roy. Soc.* **A281** (1964) 258.
17. J. HEIJBOER, *Proc. Int. Conf. Non-Crystalline Solids*, Delft 1974.

Received 14 September 1972 and accepted 1 January 1973.